HHS Public Access

Author manuscript

Adv Exp Med Biol. Author manuscript; available in PMC 2019 August 27.

Published in final edited form as:

Adv Exp Med Biol. 2019 ; 1115: 167–190. doi:10.1007/978-3-030-04278-3_8.

Cholesterol-dependent gating effects on ion channels

Qiu-Xing Jiang

Department of Microbiology and Cell Science, IFAS, University of Florida 1355 Museum Drive, Gainesville, FL 32611, USA

Abstract

Biomembranes separate a live cell from its environment and keep it in an off-equilibrium, steady state. They contain both phospholipids and nonphospholipids, depending on whether there are phosphate groups in the headgroup regions. Cholesterol (CHOL) is one type of nonphospholipids, and one of the most abundant lipid molecules in humans. Its content in plasma membranes and intracellular membranes varies and is tightly regulated. Voltage-gated ion channels are universally present in every cell and are fairly diversified in the eukaryotic domain of life. Our lipid-dependent gating hypothesis postulates that the controlled switch of the voltage-sensor domains (VSDs) in a voltage-gated potassium (Kv) channel between the “down” and the “up” state (gating) is sensitive to the ratio of phospholipids : nonphospholipids in the annular layer around the channel. High CHOL content is found to exert strong inhibitory effects on Kv channels. Such effects have been observed in *in vitro* membranes, cultured cells and animal models for cholesterol metabolic defects. Thermodynamic analysis of the CHOL-dependent gating suggests that the inhibitory effects of CHOL result from collective interactions between annular CHOL molecules and the channel, which appear to be a more generic principle behind the CHOL-effects on other ion channels and transporters. We will review the recent progress in the CHOL-dependent gating of voltage-gated ion channels, discuss the current technical limitations, and then expand briefly the learned principles to other ion channels that are known to be sensitive to the CHOL-channel interactions.

Keywords

annular lipids; cholesterol packing; bSUMs; cholesterol organization; inhibitory effects; voltage-sensor conformation

1. Introduction

All lipids in eukaryotic cell membranes contain hydrophilic headgroups and hydrophobic fatty acyl tails. They belong to two main groups --- phospholipids (group I) and nonphospholipids (group II) (Fig. 1). Group I includes glycerophospholipids and sphingomyelin phospholipids, both of which contain phosphate groups in their headgroup regions in an equivalent location. Group II includes mainly cholesterol (CHOL), glycolipids, other sphingolipids and cationic lipids. The molar ratio of phospholipids to

qxjiang@ufl.edu; jiangq9992003@yahoo.com.

nonphospholipids (PL / non-PL) varies from cell to cell or from one membrane patch to another in the same cell. In a major fraction of human cells, PL / nonPL ratio may be significantly smaller than unity, meaning that Group II lipids may be an overwhelming majority in certain cell membranes.

Group I lipids include mainly phosphatidylcholine (PC), cardiolipin, phosphatidylethanolamine (PE), phosphatidyl-glycerol (PG), phosphatidylserine (PS), phosphatidyl-inositols (PI), phosphatidic acid (PA) and sphingomyelin. Their acyl tails can vary in length and unsaturation level. Phospholipids are known to be important for the functions of specific ion channels. Anionic phospholipids, such as PS, PG, cardiolipin, PA, etc., are important for the normal function of bacterial MscL channels [4, 5]. Phosphatidyl-inositol-4, 5-bisphosphate (PIP_2) is known to regulate specific ion channels [6-12]. PG was found to be associated with the KcsA channel and important for its function [13, 14]. Crystallographic studies revealed potential phospholipid-binding sites in a Kv2.1 chimera channel and PIP_2-binding pockets in the IRK channel [15] [7]. PC content was found to be a key regulator for the topogenesis of lactose permease in bacteria [16]. Cardiolipin is a structural and functional component for the supercomplex of the electron transport chain in mitochondria [17, 18]. Because of the relative random distribution of the phospholipids in their specific leaflets of asymmetric cell membranes and the fact that nearly all known monogenic lipid metabolic defects in humans affect the cellular and systems homeostasis of nonphospholipids (group II), we will not focus our discussions on the effects of different types of phospholipids on ion channels.

Group II lipids are both structural and signaling components [19]. Fig. 1 shows the structures of four main types of Group II lipids. C40-based ether lipids, which are usually seen in extremophiles, are not diagramed here. Nor are the derivatives of cholesterol, monoacyl-glycerol, ceramides, or long unsaturated fatty acids. Diacylglycerol (DAG), a product from the hydrolysis of phosphatidylinositol 4, 5-bisphosphate (PIP2) by phospholipase C (PLC), is a second messenger that activates protein kinase C (PKC). DAG also is a ligand for MunC13, which is a critical regulator for the fusion competence of synaptic vesicles [20, 21], and an co-activator for transient receptor potential canonical (TRPC) cation channels (TRPC3/6/7) [22-25]. Cerebrosides, which include both monoglycosylceramides and oligoglycosylceramides, are important structural constituents in the plasma membranes of animal muscle and nerve cells, may cause higher phase-transition temperatures of biological membranes, and are capable for forming multi-dentate H-bonding interactions among them in order to stabilize membranes containing them [26]. Galactosylceramides are major constituents of grey matter (2% dry weight) and white matter (12% dry weight) in nervous tissues [26-28]. Cholesterol (CHOL) is literally the most abundant nonphospholipids in mammalian cells. It is the precursor for different steroid hormones. Its analogs in fungi and protozoans are called ergosterols and in plants phytosterols. *Xenopus* oocyte membranes contain ~21 mol% cholesterol [29, 30]. For the CHOL-dependent gating of voltage-gated ion channels we will discuss, animal sterols (dominantly CHOL), phytosterols and ergosterols may share strong chemical similarities. We therefore will focus on CHOL content in the plasma membranes of animal cells. The average CHOL levels in plasma membranes (PMs) are between 15 and 50 mol% whereas net content of 5–10 mol% CHOL is present in endoplasmic reticulum (ER) membranes.

However, CHOL in PMs is distributed between CHOL-poor and CHOL-rich areas, which depends on the organization of proteins and various types of lipids. In humans, brain contains ~25% of total body CHOL even though it normally accounts for merely 2–3% of body weight [31], suggesting high CHOL content in both neuronal and glial cells. CHOL affects nAChR, Kir, BK and TRPV channels [32].

Voltage-gated ion channels are a must for all cells [33]. Their dysfunction may cause severe diseases [34-46]. Except voltage-gated proton channels, all known canonical voltage-gated channels have four subunits/domains, each of which has six transmembrane segments (TMs). They contain a pore domain flanked by four VSDs (Fig. 2A). Gating of a voltage-gated channel refers to a controlled switch of its VSDs or the pore between "down" and "up" or between "closed" and "open" states, respectively. The 4^{th} TM (S4) of a VSD has evenly-spaced positively charged residues believed to move inside a *gating pore* (Fig 2B). Outer (or "upper") and inner (or "lower") crevices of the gating pore are separated by a central "hydrophobic gasket", also called the *gating charge transfer center* [1, 47]. The gating charge selectivity was proposed to rely on a conserved Phe residue, which is missing in some of the VSDs, possibly allowing structural variations in the modes of the proposed charge movements. Structures of multiple VSDs in detergents determined by X-ray or cryoEM represent "up" or "intermediately closed" states and exhibit significant structural diversity among VSDs and in the coupling of VSDs to pore domains [48-55]. Recently reported Kv structures by cryoEM further strengthened the structural diversity [52, 54, 56, 57].

Past biophysical and physiological studies have revealed abundant information about the voltage-gated ion channels at the protein level [58-62] [1, 2, 15, 50, 63-104]. Key residues contributing to voltage sensing and chemical basis for ion selectivity are established, revealing a broad range of gating charge per channel [50, 87, 105-115]. Multiple structures reveal significant differences among "up" and intermediately "down" states of the VSDs. More congruent structural features in the pore domains are established, but the allosteric coupling between VSDs and pore domains may vary strikingly (Fig. 2B) [15, 47, 50-52, 54, 56, 57, 74, 77, 87-89, 116-120]. The published data have proposed that the voltage-driven conformational changes of the VSDs may have the following components of physical movement: **1**) a simple sliding of the S4 helix "up" and "down" in the gating pore to pass individual arginine (or lysine in some channels) residues through the gating-charge transfer center, with or without possible switch of one short segment of the S4 between a regular alpha helix and a 3_{10} helix; **2**) a short sliding and rotation of the S4 helix through the focused electrostatic field across the "hydrophobic plug; **3)** the toggling of the VSDs between "outward-facing" and "inward-facing" conformations as a transporter when the tilting of helices is rearranged; **4**) the movement of S3 together with S4 and the leaning of the S1/S2 helical pairs against the S3/S4 helical pairs.

Structural studies of the VSDs from *Ciona* voltage-sensitive phosphatase (*Ci*-VSP) in two different states revealed a one-register movement (~5 Å translation and ~60° rotation) of the S4 and minor changes in the other three VSD helices, which largely accord with the intermediately "down" states seen in the NavAb and TPCs [48-50, 86]. This mode of movement, to some extent, agrees with a short vertical movement of the KvAP voltage

sensor paddle in the gating pore (not directly in lipids), an S4 movement of 6–10 Å for the focused field model, or the sliding 3_{10}-helix in the S4 by a similar distance as predicted by Rosetta modeling of the NavAb [58, 76, 77, 80, 92], even though *the structural diversity in VSDs may still allow different conformational changes to achieve functional differences*. Despite these models, a structure has so far not been available for a canonical voltage-gated ion channel that is fully kept in the resting state with all four VSDs in a complete "down" state. It is still not feasible to compare directly the VSDs of the same channel in "up" and "down" states. In the past, it has been taciturnly assumed that despite the diversified VSDs in sequence, the voltage-driven conformational changes among all, or at least a majority, of VSDs are very similar, if not identical. The structural variations in Fig. 2B, the functional diversities among various different types of voltage-gated ion channels, especially the Kv channels, and the altered gating properties of voltage-gated ion channels in different cell types or in different locations of the same cells make it plausible to consider that an alternative thinking may be needed to reconcile the different views of the voltage-gating mechanisms. Lipid-dependent gating hypothesis represents a new proposal in this direction.

2. Overview of CHOL-effects on voltage-gated ion channels

As integral membrane proteins, Kv channels are expected to be sensitive to their lipid environments. When *Xenopus* oocytes were used as a heterogeneous expression system for Kv channels and cell-attached patches were formed to record channel activity, it has been long known that functional Kv channels on the surface of the oocytes appear clustered in hot spots, especially in regions of the animal pole that are close to the boundary between the dark-colored animal pole and the faintly-colored vegetal pole. When a pore-blocking toxin, CTX or AgTx2, was mutated and conjugated with a nanogold particle, and used to detected *Shaker* K channel on the surfaces of Xenopus oocytes, it was observed that the channels were randomly distributed on the surfaces (QXJ, unpublished observations). Similar observations of nonfunctional voltage-gated ion channels were made on the surface of cultured cells and neurons. These could be attributed either to channel proteins that were not fully matured or to the lipid environments in cell membranes [121, 122]. For example, Kv2.1 is delivered to different regions of a neuronal cell, but only a fraction of the channels are functional when patched by cell-attached patches. When expressed in cultured cells, the Kv2.1 channels in puncta, which refer to microdomains that consist of both proteins and special lipids, are usually not active [123, 124]. Phosphorylation and dephosphorylation was proposed as a possible mechanism. In view of the strong lipid-dependent gating effects and well-known or characterized cholesterol-rich domains, it is very likely that the special lipids around the proteins might contribute to the inhibitory effects on the channel activity [124].

Chemical treatments to alter CHOL content led to either inhibitory or stimulatory effects on voltage-gated ion channels [125-140]. The partial or nearly complete depletion of CHOL with methyl-β-cyclodextrin (MBCD) in different cells has caused different effects. Changes in current density, activation / deactivation kinetics, inactivation rate, and shifts in G-V relation were reported. For example, 1 mM MBCD treatment of NG108–15 neurons overexpressing Kv3.1 channels led to slower activation / deactivation and decrease in firing frequency of action potential (AP's) [126]. Contrastingly, in rat hippocampal neurons, MBCD treatment increased the firing frequency of AP's by increasing the current density of

delayed rectifier Kv channels and accelerating the activation and deactivation of the A-type Kv channels [128]. The opposite effects for different Kv channels in neurons and other cells have been puzzling. On the other hand, MBCD treatment has been demonstrated to cause severe structural changes in cells. 1–3 mM MBCD treatment of mouse fetal skeletal muscle cells for 1 hour at 37 °C caused obvious decrease in caveolae and T-tubule area [133]. *Such complications from chemical treatment raised serious concerns and cast strong doubt on all past data collected from voltage-gated ion channels in MBCD-treated cells.*

More consistent data, however, were obtained in cells loaded with MBCD-CHOL, where the inhibitory effects of higher CHOL content were observed for L-type Ca^{2+} channels (Cav1.2) in mouse fetal skeletal muscle cells [133], Kv1.3 in T lymphocytes [129, 134, 138], L-type Ca^{2+} channels in coronary artery smooth muscle cells [141], Kv11.1 in adult canine ventricular myocytes [142], and Kv channels in coronary arteriolar smooth muscle cells [141]. The main reason for such consistency among different channels in cultured cells or in primary tissues is probably attributable to intrinsic effects of high content of CHOL and its analogs on membrane stability and the voltage-gated ion channels, which could only be quantitatively studied in a well-controlled membrane system.

3. Lipid-dependent gating predicts strong CHOL-dependent inhibition of Kv channels.

My laboratory started the investigation of the lipid-dependent effect in a well-controlled system, where the channels were completely pure and the lipids in defined composition formed fluidic membranes. Under such conditions, we first discovered that the phosphate groups in the lipid bilayers were essential for a Kv channel to reach its open state [75], which was echoed by findings from Dr. Zhe Lu's lab where sphingomyelinases were used to treat cell membranes and alter activities of various eukaryotic Kv channels [143, 144]. After carefully studying the conformational states of both the voltage-sensor domains and the channel pore in different lipids, we concluded that in homogeneous membranes, Group II lipids favor the KvAP in a resting state with its VSDs in the "down" conformation. Moreover, the lipid-stabilized "resting" state is equivalent or tightly connected to the native one driven by hyperpolarization in transmembrane electrostatic potential [145], leading to our hypothesis of **"lipid-dependent gating"** (Fig. 3) [146]. Physicochemically, we may speculate that the lipid-dependent gating mainly stems from the nonphospholipids in the annulus around a channel. These lipids cause energetic difference between different gating states of the VSDs. This hypothesis explains partial gating charge immobilization caused by sphingomyelinase treatment of cells [143] and may explain the clusters of nonconducting Kv channels in cholesterol-rich domains in cultured cells [122] or gating charge immobilization of the Kv4.3 channels in midbrain dopamine neurons directly caused by endocannabinoids (besides faster inactivation effect) [147]. Similar lipid-dependent conformational changes in the VSDs were reported for hyperpolarization-activated MVP channels [148].

Studies by my laboratory and later by other groups in other channels suggest a self-coherent explanation for various lipid effects we have observed. There is thus a good reason to believe

that our hypothesis of lipid-dependent gating may underlie a more general inhibitory effect of nonphospholipids on Kv channels. Among all the Group II lipids, CHOL is probably the most studied because of its importance to public health and the available technologies and reagents in analyzing CHOL in different cells and tissues. The lipid-dependent gating hypothesis predicts that CHOL exerts strong inhibitory effects on a variety of eukaryotic Kv channels. We will call this prediction **the CHOL-dependent gating of Kv channels**. As reported before, hypercholesterolemia caused inhibitory effects on Cav2.1 channels in coronary arterial smooth muscle cells [136]. The CHOL-dependent gating effects may be expanded to both Cav and voltage-gated Na^+ (Nav) channels, depending on the accessibility of their VSDs [149]. On the other hand, such gating effects might be less prominent for voltage-gated Na^+ (Nav) or Ca^{2+} (Cav) channels [125-140], probably because eukaryotic Nav and Cav have four different VSDs and their VSDs may be shielded (at least partially) from annular lipids by auxiliary transmembrane subunits [55, 96, 150, 151]. Recent results did show that Nav1.9 in DRG neurons could be relieved from CHOL-dependent inhibition when inflammation lowers cholesterol content in these neurons and causes Nav1.9 to be repartitioned from “CHOL-rich lipid rafts to CHOL-poor non-raft regions” [149]. It is therefore necessary to take into account potential complications from channel proteins, accessory proteins and lipid environments when we apply the lipid-dependent gating effects to experimental observations.

4. Cholesterol distribution in membranes and cholesterol-dependent phase separation

As a key component in cell membrane, CHOL may be equally or asymmetrically distributed between two leaflets. Even though the small polar headgroup (-OH) of CHOL allows relatively easy flipping across the hydrophobic core, transbilayer asymmetry of CHOL has been observed in plasma membranes of different mammalian cells due to active transport from the inner to the outer leaflet and the retention of CHOL in the outer leaflet [152]. The cholesterol content in plasma membranes of a cell may vary in the range of 15 to 50 mol%. Presence of CHOL fills in crevices between packed fatty acyl tails in the hydrophobic region and leaves gaps in the layer of the headgroups such that CHOL-rich membranes tend to have smooth phase transition, instead of a sharp switch from the fluidic phase to the crystalline gel phase during cooling. The gaps left by CHOL molecules in the headgroup layer are believed to increase the disorder of the headgroup layer.

Preferential packing of CHOL and sphingomyelin (SPhM) has been proposed to form dynamic lipid rafts in membranes or more stable structures like caveolae [153-157]. Super-resolution imaging suggests that the dynamic lipid rafts might be of 120–150 nm in diameter in cell membranes [158]. Secondary Ion Mass Spec (SIMS) imaging indeed failed to detect large structures made by co-clustering of sphingomyelin and CHOL [159, 160]. Physicochemical studies also showed that in a ternary system made of PC/SPhM/CHOL, all lipids might be organized into a CHOL-sparse phase with individual CHOL-rich islands [161, 162]. CHOL-dependent gating thus depends on the distribution of voltage-gated ion channels in the CHOL-rich domains, CHOL-sparse phase, or the boundary between the two.

Unfortunately with current super-resolution fluorescence microscopy or high-resolution cryo-electron microscopy, it is still not possible to discern individual lipid molecules around each ion channel in a cell membrane. Quantitative analysis of CHOL-dependent gating thus requires a homogeneous system, which allows more precise control of lipid composition, CHOL content, phase behavior, channel density and orientation. We developed a bead-supported unilamellar membrane system (bSUM) in order to achieve these effects (Fig. 4). In this system, a high density of surface ligands on a bead is used to sequester and select affinity-tagged channel proteins. The bSUM is advantageous in several aspects: **a)** A majority of channels are in the same orientation; **b)** Channels mediate the formation of the lipid bilayer; **c)** There is one and only one bilayer; **d)** Lipids are changeable and the bead sizes can be controlled from 0.1 to 20 μm; **e)** Channels can be recorded by patch clamp; **f)** Fast voltage-clamp speed (0.2–0.5 ms) is suitable for studying Kv channels with fast kinetics; **g)** It is suitable to measure the fluidity or phase separation in the membranes. Because of the fast gating kinetics of Nav, Cav and many eukaryotic Kv channels, bSUMs will be better than almost all of the other *in vitro* membrane systems, such as bilayer membranes, glass-supported biomembrane, etc., and more stable than giant unilamellar vesicles (GUVs).

Cholesterol differs from phospholipids in another peculiar aspect. Chemical structures showed in Fig 2 suggest that the electronegative OH group endows partial positive charges at the hydrophobic terminus of cholesterol. The stronger ester groups in a phospholipid for linking the fatty acyl chains endow higher partial positive charges to the hydrophobic core than a cholesterol molecule. It means that with the incorporation of more cholesterol, the positive potential in the middle of a regular phospholipid bilayer would become weakened. A decrease of the hydrophobic core dipole potential from ~+500 mV to ~+200 mV in the membrane might be a contributing factor to favor the VSDs of a Kv channel in a specific gating state [163]. Such an effect has not been studied, and still awaits future investigations.

5. A thermodynamic model for lipid-channel interactions

A canonical gating model for the *Shaker* K^+ channel can be used to address the energetics behind the CHOL-dependent gating effects (Fig 5). In this model, the switch of four VSDs from the “down” to the “up” state must happen first before a concerted coupling of the VSDs and the pore domain that leads to the pore opening ($C_x \rightarrow O$) [112]. We assume that all the low affinity binding sites for the CHOL molecules in the annular layer of lipids next to the channel remain even though these sites may change their affinity during the gating transition. The general ON-rate (the activation rate) for channel opening represents the allosteric change from a close state to the open state. The ON-rate is dominated by the rate-limiting step or the combination of a few steps that together determine the apparent rate of voltage-dependent activation. The OFF-rate for closing the open channel is defined by a combination of the kinetic constants for the two pathways that are connected to the O state. The OFF-rate can be determined from the mean life-time of the O state, assuming there is one and only one open state here.

CHOL-dependent inhibition of the channel activity is ultimately to shift the channels away from the two open states --- the O and O.L states. Collectively, the difference in free energy

change *(ΔΔG)* between the closed states and the open states is resulted from the binding of CHOL to multiple sites on probably different subunits with similar or quite different affinities for CHOL. Based on the dimension of a Kv channel and the diameter of a typical lipid molecule, there is enough space for ~ 120 lipid molecules in the annular layer next to each channel. A significant ΔΔG may come from a combination of a few high-affinity binding sites and / or low-affinity binding sites among the ~10 mol% CHOL among these annular lipids if each CHOL contributes an energetic difference of ~3 kT, which is equivalent to merely a 3–8 fold change in the apparent binding affinity at each binding site. The summed energetic change of ~25 kT is sufficient to cause a significant shift of the Q-V (gating charge versus membrane potential) or G-V (relative conductance versus membrane potential) curve by 100–200 mV with an apparent gating charge similar to a *Shaker*-like K channel, which has a total gating charge of 10–13 elementary charges, and an apparent charge of ~4 elementary charges from its G-V relation. Such a consideration suggests that a small change in binding affinity for multiple CHOL-binding sites together can cause a major shift in G-V and Q-V.

More numerical calculations for the kinetic model will not be presented here. Instead, we will use the macroscopic $k_{on}(V) / k_{off}(V)$ to reach a conceptual understanding. The rate-limiting forward step leading to the opening of the channel and the rating-limiting deactivation step will dominate the distribution of the channels between the closed states and the open state. CHOL binding to multiple low-affinity binding sites may decrease the $k_{on}(V) / k_{off}(V)$ and exert strong inhibitory effects on the channel opening, and disfavor the activated state (Fig. 3). The scheme in Fig. 5 may make it more complicated if the cholesterol effect is caused by the energetic difference in the switching of the VSDs. It might cause a similar increase in $k_{on}(V)$ *and* $k_{off}(V)$*, leading to only small apparent shift of G-V, but a decrease in open channel activity (current density) through changes in open probability and dwell time for the open-state*. Direct measurement of VSDs movement will be needed in such cases.

Because the details in the gating scheme may differ among the various Kv channels, especially the rate-limiting steps in the forward transition, the possible subconductance steps, the inactivation steps, and the movement of the VSDs in different lipid conditions, it is expected that the inhibitory effects of CHOL-dependent gating may be manifested differently when we compare the activation / deactivation / inactivation rates, the G-V / Q-V curve shifts, the open probability and dwell-time of open states, the steady-state currents after inactivation, etc. Other complicating factors such as channel density, lipid composition around individual channels, cell conditions under chemical modifications or genetic manipulations, etc. may also complicate the effects. These considerations will be necessary when direct lipid-channel interactions are used to account for CHOL-dependent gating or lipid-dependent gating in cell membranes.

6. Kv-channels are sensitive to cholesterol content

The above considerations make it important to use a well-controlled system to study the fundamental principles behind the CHOL-dependent gating without the interferences from uncontrolled factors in cellular environments. We initially used a solvent-based planar lipid

bilayer system, and found that a small amount of CHOL likely introduced significant inhibitory effects [145]. The lipid bilayer system has three limits. 1) It was difficult to control the fusion of CHOL-containing vesicles with the bilayer membrane; 2) The chemical nature of CHOL might drive its selective partition into the solvent (decane) islands or annulus in a bilayer membrane; and 3) The clamp speed is slow such that channel activity with fast gating kinetics can not be resolved well. These limitations might have contributed to the observations by Finol-Urdaneta et al, who detected no CHOL-dependent gating when fusing KvAP channels in PE/PG vesicles into bilayer membranes made of PE/PG/CHOL, due to possible partition of cholesterol into the decane phases [127].

Our bSUMs were developed in order to overcome these technical limitations [3], and we were able to control CHOL content in membranes using a predefined molar ratio (mol%). With ~10 mol% CHOL, KvAP only started to show activity when the membrane potential (V_m) was > +60 mV [3]. Studies of DOPC/CHOL membranes showed that 9.6 mol% CHOL membrane is highly fluidic [164]. The channel identity was verified with a 33H1Fv, which was derived from a monoclonal antibody. The reconstitution process removed all detergents and achieved random insertion of both CHOL and DOPC into the bSUMs, which allows the predefinition of DOPC/CHOL ratio. Comparing the G-V curves of KvAP in DOPC with 4.0 and 9.6 mol% CHOL (Fig. 6A vs 6B) revealed significant shifts, which are +210 mV in 9.6 mol% CHOL and +160 mV in 4.0 mol% (brown and red traces in Fig. 6C). Consistent with our hypothesis, 9.6 ml% CHOL stabilized KvAP in a closed state by ~18 *kcal/mol, using the apparent gating charge of 4.0 elementary charges*. Such a free energy change *(ΔΔG*) could only be partially accounted for by changes in ON- and OFF-rates (~3.3 *kcal/mol*; not shown), suggesting that CHOL effects on VSDs probably dominate the stabilizing effect, which differs from the proposed replacement of phospholipids bound at the S4/S5 linkers to affect the concerted opening step during activation [11, 140]. In a homogeneous membrane, the CHOL effect is much stronger than what was reported in chemically treated cells [132, 134], which were probably lessened by the presence of CHOL-free domains, changes in types and levels of membrane proteins, vesicle fusion or endocytosis. Without these complications, our analysis in bSUMs is direct and more accurate and quantitative.

7. Genetic mutations that affect cholesterol content in cell membranes

Virtually all human lipid metabolic defects affect Group II lipids [165], and all may cause severe neurological defects and early death [166-168]. Recently in the acutely isolated dopaminergic neurons, it was found that the endocannabinoids and its analogs directly inhibit Kv4.3 channels by altering the inactivation rate and causing partial immobilization of gating charge [147]. The endocannabinoids are analogs of Group II lipids, and their effects suggest that distribution of the Group II lipids or their analogs around the channels is important to the cholesterol-dependent gating.

There are three pathways for cholesterol homeostasis in a human cell: uptake of LDL particles from outside, de novo synthesis of cholesterol in the ER, and the recycling of cholesterol from lysosome to the plasma membranes. Autophagosomes may contribute to the recycling pathway. There are different knockout mouse models for multiple genes in the pathway for cholesterol synthesis. Nonfunctional enzymes for cholesterol synthesis will lead

to the decrease of cholesterol level in ER and ultimately in other cell membranes. NPC1 and NPC2 are the two enzymes responsible for the recycling of cholesterol[169, 170]. Their malfunction leads to severe lysosome-storage disease due to the accumulation of cholesterol in the lysosomes and autophagolysosomes. In cultured cells, knockout NPC1 and NPC2 leads to significant lower cholesterol content. In knockout mice, both NPC1 and NPC2 cause severe neurological symptoms, mirroring the severe neurological phenotypes in human patients[171]. The LDL-uptake is achieved through receptor-mediated endocytosis. Disruption of one or more of the three pathways will decrease cholesterol content in cell membranes and exert strong effects on at least some of the voltage-gated ion channels by removing part of the CHOL-dependent inhibition. The decreased cholesterol content in plasma membranes has the potential to cause higher activity of Kv channels and in turn lower excitability in the neurons that are affected. If such effects are more prominent in the inhibitory pathways, the net effect will become excitatory and cause hyperexcitability. Studies of Kv channels in cultured cells or knockout mice with defects in the three pathways will provide important information on the physiological significance of the CHOL-dependent gating of Kv channels in the future.

Structural comparison in Fig. 2 of the nonphospholipids and phospholipids suggests that there is a special role of the phosphate layer in shaping the electrostatic field across the bilayer, which has not been well understood. In the current molecule dynamics model, the difference between the DOTAP membrane and the DOPC bilayer was thought to be trivial because the salts in solution appeared sufficient to shield the effects of phosphates [172]. But the experimental difference was very dramatic when a voltage-gated channel (or its VSDs) was used as a lipid sensor. Without a good atomistic model for these two types of lipids, calculations for energetic difference of any protein in them would fail to certain extent. The nature of the force field for the two groups of lipids might need to be better defined in order to make good testable predictions. Quantum mechanical treatment of the atoms around the phosphodiesters plus molecular dynamics will be a possible avenue in understanding the role of phosphates in distinguishing the Group I and II lipids.

8. Kv channels as sensors for changes in cholesterol content

Our studies of KvAP in bSUMs (Fig. 6) demonstrated significant sensitivity of the VSDs to changes in CHOL-content. In eukaryotic systems, multiple Kv channels have been found to be co-localized with marker proteins for lipid-rafts or caveolae [133, 173-175]. The Kv channels in cholesterol-rich domains are expected to experience significant inhibitory effects. It appears that the Kv channels are much more sensitive because all four VSDs must undergo significant conformational changes in order to gate the channel pore and all VSDs are directly exposed to annular lipids (CHOL). No previous study has been able to determine specific factors that affect the delivery of a Kv channel into the CHOL-rich domains. Nor has it been possible to count the channels in CHOL-rich domains, CHOL-poor phases and the boundary between them.

From an evolutionary viewpoint, our hypothesis predicts that the diversified sequences of Kv channels, especially the VSD sequences, and the distribution of various Kv channels in different cells with contrastingly different lipids may reflect the co-evolution of specific Kv

channels and the lipid environments in specific cells. For example, the lipid composition of the plasma membranes in a glial cell, a neuron and an adipocyte is known to be fairly different. A glial cell has high content of plasmalogens [176]. A neuronal cell harbors high level of gangliosides. An adipocyte contains a large fraction of surface area covered by caveolae. Kv channels in these cells are expected to experience contrastingly different lipid environments and therefore may manifest the CHOL-dependent gating effects to different extents. It might be feasible to transduce these cells with a viral vector to overexpress Kv2.1 or other channels in order to study their gating property in different regions of the cell membranes.

On the other hand, the current patch clamp techniques and imaging methods are not sufficient to reveal the annular lipids around individual channels. Other methods need to be tested. For example, a combination of super-resolution imaging of fluoresterol or other probes for CHOL and a labeled Kv channel (say Kv2.1) with cell-attached patch clamp recordings using a small-bore electrode will likely be suitable to reveal new insights on the direct distribution of cholesterol around a small number of Kv channels in cells. But the limited resolution at 50–200 nm is not able to reach single lipid resolution. Cryo-EM analysis of individual channels will need to average images of hundreds or thousands of ion channels in order to reveal the positions of stably bound structural lipids, not necessarily the lipids that are involved in gating modulation [177]. Secondary Ion Mass Spectrometry is not able to reach single-lipid resolution for imaging individual lipids, either. Molecular Dynamic simulations using better force field to account for the differences between Group I and Group II lipids may be feasible in the near future. A completely new experimental method is thus needed in order to reach high-resolution imaging of annular lipids around individual channels. It is speculated that exposure to high-brilliance beam of either X-ray or electrons will potentially allow the structure determination for small membrane patches from a high-density sample of Fourier components.

9. Other ion channels that are sensitive to change in cholesterol content

Ion channel sensitivity to CHOL content has been more extensively studied for nAChR (nicotinic acetylcholine receptor) and G-protein-gated inward rectifier K channel (GIRK) [32, 178-181]. nAChR has an annular CHOL at the interface between M4 and M1+M3, in proximity to the pore-lining M2 transmembrane helix. The M4 lipid sensor model proposes that the binding of lipids at the M4 site in the outer leaflet has direct effects on the transition of the channel into an uncoupling state. Cryo-EM averaging revealed recently potential empty spaces at the M1 and M4 interface for an annular CHOL in the outer leaflet, consistent with the M4 lipid sensor model deduced from the functional studies, even though still being complicated by uncertainty in averaging out the density for a disordered headgroup [177]. Further the bound lipids are proposed to exert strong gating control to the channel. DAG was proposed to be a strong nAChR activator, which might be able to account for the empty space in the cryoEM density equally well. The biophysical nature of the CHOL- and DAG-binding in terms of their positions and functional effects on ion channels needs further characterization.

For GIRK interaction with CHOL in a stereo-sensitive manner, there are a few recent reviews discussing high-affinity binding sites based on structural studies [32]. CHOL-binding acts mainly as an agonist in potentiating the function, and as an antagonist in a few cases. The “principal” CHOL-binding site in the crevice between the TM1 and TM2 in the outer leaflet is in proximity to the selectivity filter. The “transient” binding site in the inner leaflet is next to the inner gate and the coupling site at the intracellular surface, close to the PIP2-binding site. In consideration of the relatively equal distribution of cholesterol in both leaflets, it is likely that these identified CHOL-binding sites will play a significant role when the channels are relocated between CHOL-rich and CHOL-poor regions in cell membranes.

In both nAChR and IRKs, CHOL-binding is in close coupling to the gate of the channel pore and the stability of the open state. It is not expected that CHOL-binding or unbinding would cause major conformational changes despite the proposed M4-movement for the nAChR after cholesterol-binding. This view is fairly different from the proposed conformational changes of the VSDs in the Kv channels (Fig 3).

Many other channels may have direct sensors for the annular lipids. Nav1.9 channels were recently identified as a sensor for plasma membrane cholesterol in DRG (dorsal root ganglion) neurons that sense inflammatory pain. The pain sensitivity was higher when Nav1.9 channels were redistributed from CHOL-rich domains to CHOL-poor ones [149]. TRPV1 was found to have stably-bound lipids in the nano-discs which do not have a complete annular layer of lipids [182]. It would be interesting the study the lipid-dependent gating of TRPV1 in a well-controlled lipid environment, such as the bSUMs, or in native cell membranes after genetic manipulations of lipid homeostasis of the neurons. The same is probably true for multiple other TRPs, especially those that function in plasma membranes and lysosomal membranes.

10. General conclusions and future perspectives.

The lipid-dependent gating is probably a more general steady-state gating modality for voltage-gated ion channels. The chemical treatment by MBCD-CHOL to increase CHOL content has shown consistent inhibitory effects on different voltage-gated ion channels in different cells, all of which agree with the strong inhibitory effects observed in bSUMs (Fig. 6). The depletion of CHOL by MBCD is expected to cause severe structural heterogeneity and functional changes in cells and may alter channel density and its delivery to or retrieval from the cell membrane. Voltage-gated ion channels are thus adapted to their physiological lipid environments, and sensitive to changes in lipid composition caused by lipid metabolic defects in their native niches, some of which result in significant changes in the gating properties of voltage-gated ion channels and severe pathological phenotypes. Multiple low-affinity binding sites in the annular layer are sufficient to exert strong collective effects and change the gating property of a Kv channel. So far we still lack a high-resolution tool to reveal the dynamic interactions between annular CHOL and voltage-gated ion channels. Structural studies of a Kv channel in a CHOL-rich bilayer membrane may provide a direct view in the future.

Acknowledgements:

Over the years the main body of research in my laboratory on lipid-dependent gating has been funded by NIH (R01GM111367, R01GM093271 & R01GM088745), AHA (12IRG9400019), CF Foundation (JIANG15G0), Welch Foundation (I-1684) and CPRIT (RP120474). I am indebted to many colleagues in the ion channel field and in lipid research for their valuable suggestions and advice. I have tried my best to cover most, if not all, published work closely related to CHOL-dependent gating effects on ion channels, and would apologize to those whose work is not cited here.

References:

1. Li Q, et al., Structural mechanism of voltage-dependent gating in an isolated voltage-sensing domain. Nat Struct Mol Biol, 2014 21(3): p. 244–52. [PubMed: 24487958]
2. Long SB, Campbell EB, and Mackinnon R, Crystal structure of a mammalian voltage-dependent Shaker family K+ channel. Science, 2005 309(5736): p. 897–903. [PubMed: 16002581]
3. Zheng H, et al., bSUM: A bead-supported unilamellar membrane system facilitating unidirectional insertion of membrane proteins into giant vesicles. J Gen Physiol, 2016 147(1): p. 77–93. [PubMed: 26712851]
4. Powl AM, East JM, and Lee AG, Anionic phospholipids affect the rate and extent of flux through the mechanosensitive channel of large conductance MscL. Biochemistry, 2008 47(14): p. 4317–28. [PubMed: 18341289]
5. Powl AM, East JM, and Lee AG, Lipid-protein interactions studied by introduction of a tryptophan residue: the mechanosensitive channel MscL. Biochemistry, 2003 42(48): p. 14306–17. [PubMed: 14640699]
6. Zaydman MA, et al., Kv7.1 ion channels require a lipid to couple voltage sensing to pore opening. Proc Natl Acad Sci U S A, 2013 110(32): p. 13180–5. [PubMed: 23861489]
7. Whorton MR and MacKinnon R, X-ray structure of the mammalian GIRK2-betagamma G-protein complex. Nature, 2013 498(7453): p. 190–7. [PubMed: 23739333]
8. Rittenhouse AR, PIP2 PIP2 hooray for maxi K+. J Gen Physiol, 2008 132(1): p. 5–8. [PubMed: 18562503]
9. Lee J, et al., PIP2 activates TRPV5 and releases its inhibition by intracellular Mg2+. J Gen Physiol, 2005 126(5): p. 439–51. [PubMed: 16230466]
10. Xiao J, Zhen XG, and Yang J, Localization of PIP2 activation gate in inward rectifier K+ channels. Nat Neurosci, 2003 6(8): p. 811–8. [PubMed: 12858177]
11. Zaydman MA and Cui J, PIP2 regulation of KCNQ channels: biophysical and molecular mechanisms for lipid modulation of voltage-dependent gating. Front Physiol, 2014 5: p. 195. [PubMed: 24904429]
12. Furst O and D'Avanzo N, Isoform dependent regulation of human HCN channels by cholesterol. Sci Rep, 2015 5: p. 14270. [PubMed: 26404789]
13. Valiyaveetil FI, Zhou Y, and MacKinnon R, Lipids in the structure, folding, and function of the KcsA K+ channel. Biochemistry, 2002 41(35): p. 10771–10777 3149. [PubMed: 12196015]
14. Valiyaveetil FI, et al., Glycine as a D-amino acid surrogate in the K(+)-selectivity filter. Proc Natl Acad Sci U S A, 2004 101(49): p. 17045–9. [PubMed: 15563591]
15. Long SB, et al., Atomic structure of a voltage-dependent K+ channel in a lipid membrane-like environment. Nature, 2007 450(7168): p. 376–82. [PubMed: 18004376]
16. Dowhan W and Bogdanov M, Lipid-dependent membrane protein topogenesis. Annu Rev Biochem, 2009 78: p. 515–40. [PubMed: 19489728]
17. Zhang M, Mileykovskaya E, and Dowhan W, Cardiolipin is essential for organization of complexes III and IV into a supercomplex in intact yeast mitochondria. J Biol Chem, 2005 280(33): p. 29403–8. [PubMed: 15972817]
18. Mileykovskaya E, Zhang M, and Dowhan W, Cardiolipin in energy transducing membranes. Biochemistry (Mosc), 2005 70(2): p. 154–8. [PubMed: 15807653]
19. Alberts B, et al., Molecular Biology of the Cell. 5th ed. 2007, New York: Galand Science.

20. Palfreyman M and Jorgensen EM, PKC defends crown against Munc13. Neuron, 2007 54(2): p. 179–80. [PubMed: 17442237]
21. de Jong AP, et al., Phosphorylation of synaptotagmin-1 controls a post-priming step in PKC-dependent presynaptic plasticity. Proc Natl Acad Sci U S A, 2016 113(18): p. 5095–100. [PubMed: 27091977]
22. Kalwa H, et al., Phospholipase C epsilon (PLCepsilon) induced TRPC6 activation: a common but redundant mechanism in primary podocytes. J Cell Physiol, 2015 230(6): p. 1389–99. [PubMed: 25521631]
23. Zhang X and Trebak M, Transient receptor potential canonical 7: a diacylglycerol-activated non-selective cation channel. Handb Exp Pharmacol, 2014 222: p. 189–204. [PubMed: 24756707]
24. Itsuki K, et al., PLC-mediated PI(4,5)P2 hydrolysis regulates activation and inactivation of TRPC6/7 channels. J Gen Physiol, 2014 143(2): p. 183–201. [PubMed: 24470487]
25. Venkatachalam K, Zheng F, and Gill DL, Control of TRPC and store-operated channels by protein kinase C. Novartis Found Symp, 2004 258: p. 172–85; discussion 185–8, 263–6. [PubMed: 15104182]
26. Schmitt S, Castelvetri LC, and Simons M, Metabolism and functions of lipids in myelin. Biochim Biophys Acta, 2015 1851(8): p. 999–1005. [PubMed: 25542507]
27. Smaby JM, et al., Cholesterol-induced interfacial area condensations of galactosylceramides and sphingomyelins with identical acyl chains. Biochemistry, 1996 35(18): p. 5696–704. [PubMed: 8639529]
28. Di Biase A, Salvati S, and Serlupi Crescenzi G, Lipid profile of rat myelin subfractions. Neurochem Res, 1990 15(5): p. 519–22. [PubMed: 2370944]
29. Hill WG, et al., Isolation and characterization of the Xenopus oocyte plasma membrane: a new method for studying activity of water and solute transporters. Am J Physiol Renal Physiol, 2005 289(1): p. F217–24. [PubMed: 15741609]
30. Sadler SE, Low-density caveolae-like membrane from Xenopus laevis oocytes is enriched in Ras. J Cell Biochem, 2001 83(1): p. 21–32. [PubMed: 11500951]
31. Orth M and Bellosta S, Cholesterol: its regulation and role in central nervous system disorders. Cholesterol, 2012 2012: p. 292598. [PubMed: 23119149]
32. Levitan I, Singh DK, and Rosenhouse-Dantsker A, Cholesterol binding to ion channels. Front Physiol, 2014 5: p. 65. [PubMed: 24616704]
33. Hille B, Ion Channels of Excitable Membranes. 3rd ed. 2001, Sunderland, MA, USA: Sinauer Associates, Inc.
34. Shribman S, et al., Voltage-gated potassium channelopathy: an expanding spectrum of clinical phenotypes. BMJ Case Rep, 2013 2013.
35. Poolos NP and Johnston D, Dendritic ion channelopathy in acquired epilepsy. Epilepsia, 2012 53 Suppl 9: p. 32–40. [PubMed: 23216577]
36. Baig SM, et al., Loss of Ca(v)1.3 (CACNA1D) function in a human channelopathy with bradycardia and congenital deafness. Nat Neurosci, 2011 14(1): p. 77–84. [PubMed: 21131953]
37. Xie G, et al., A new Kv1.2 channelopathy underlying cerebellar ataxia. J Biol Chem, 2010 285(42): p. 32160–73. [PubMed: 20696761]
38. Tremblay J and Hamet P, Genetics of pain, opioids, and opioid responsiveness. Metabolism, 2010 59 Suppl 1: p. S5–8. [PubMed: 20837195]
39. Pietrobon D, CaV2.1 channelopathies. Pflugers Arch, 2010 460(2): p. 375–93. [PubMed: 20204399]
40. Rajakulendran S, et al., Episodic ataxia type 1: a neuronal potassium channelopathy. Neurotherapeutics, 2007 4(2): p. 258–66. [PubMed: 17395136]
41. Kordasiewicz HB and Gomez CM, Molecular pathogenesis of spinocerebellar ataxia type 6. Neurotherapeutics, 2007 4(2): p. 285–94. [PubMed: 17395139]
42. Howard RJ, et al., Structural insight into KCNQ (Kv7) channel assembly and channelopathy. Neuron, 2007 53(5): p. 663–75. [PubMed: 17329207]
43. Estevez M, Invertebrate modeling of a migraine channelopathy. Headache, 2006 46 Suppl 1: p. S25–31. [PubMed: 16927961]

44. Cox JJ, et al., An SCN9A channelopathy causes congenital inability to experience pain. Nature, 2006 444(7121): p. 894–8. [PubMed: 17167479]
45. Bjerregaard P, Jahangir A, and Gussak I, Targeted therapy for short QT syndrome. Expert Opin Ther Targets, 2006 10(3): p. 393–400. [PubMed: 16706679]
46. Poolos NP, The h-channel: a potential channelopathy in epilepsy? Epilepsy Behav, 2005 7(1): p. 51–6. [PubMed: 15961349]
47. Tao X, et al., A gating charge transfer center in voltage sensors. Science, 2010 328: p. 67–73. [PubMed: 20360102]
48. Kintzer AF and Stroud RM, Structure, inhibition and regulation of two-pore channel TPC1 from Arabidopsis thaliana. Nature, 2016 531(7593): p. 258–62. [PubMed: 26961658]
49. Guo J, et al., Structure of the voltage-gated two-pore channel TPC1 from Arabidopsis thaliana. Nature, 2016 531(7593): p. 196–201. [PubMed: 26689363]
50. Payandeh J, et al., The crystal structure of a voltage-gated sodium channel. Nature, 2011 475(7356): p. 353–8. [PubMed: 21743477]
51. Wang W and MacKinnon R, Cryo-EM Structure of the Open Human Ether-a-go-go-Related K+ Channel hERG. Cell, 2017 169(3): p. 422–430 e10. [PubMed: 28431243]
52. Lee CH and MacKinnon R, Structures of the Human HCN1 Hyperpolarization-Activated Channel. Cell, 2017 168(1–2): p. 111–120 e11. [PubMed: 28086084]
53. Hite RK and MacKinnon R, Structural Titration of Slo2.2, a Na+-Dependent K+ Channel. Cell, 2017 168(3): p. 390–399 e11. [PubMed: 28111072]
54. Whicher JR and MacKinnon R, Structure of the voltage-gated K(+) channel Eag1 reveals an alternative voltage sensing mechanism. Science, 2016 353(6300): p. 664–9. [PubMed: 27516594]
55. Wu J, et al., Structure of the voltage-gated calcium channel Cav1.1 complex. Science, 2015 350(6267): p. aad2395. [PubMed: 26680202]
56. Wang W and MacKinnon R, Cryo-EM Structure of the Open Human Ether-a-go-go-Related K(+) Channel hERG. Cell, 2017 169(3): p. 422–430 e10. [PubMed: 28431243]
57. Sun J and MacKinnon R, Cryo-EM Structure of a KCNQ1/CaM Complex Reveals Insights into Congenital Long QT Syndrome. Cell, 2017 169(6): p. 1042–1050 e9. [PubMed: 28575668]
58. Vargas E, et al., An emerging consensus on voltage-dependent gating from computational modeling and molecular dynamics simulations. J Gen Physiol, 2012 140(6): p. 587–94. [PubMed: 23183694]
59. Villalba-Galea CA, et al., Charge movement of a voltage-sensitive fluorescent protein. Biophys J, 2009 96(2): p. L19–21. [PubMed: 19167283]
60. Vargas E, Bezanilla F, and Roux B, In search of a consensus model of the resting state of a voltage-sensing domain. Neuron, 2011 72(5): p. 713–20. [PubMed: 22153369]
61. Villalba-Galea CA, et al., S4-based voltage sensors have three major conformations. Proc Natl Acad Sci U S A, 2008 105(46): p. 17600–7. [PubMed: 18818307]
62. Chanda B and Bezanilla F, A common pathway for charge transport through voltage-sensing domains. Neuron, 2008 57(3): p. 345–51. [PubMed: 18255028]
63. Bezanilla F, The voltage-sensor structure in a voltage-gated channel. Trends Biochem Sci, 2005 30(4): p. 166–8. [PubMed: 15817390]
64. Sigg D and Bezanilla F, A physical model of potassium channel activation: from energy landscape to gating kinetics. Biophys J, 2003 84(6): p. 3703–16. [PubMed: 12770877]
65. Bezanilla F and Perozo E, The voltage sensor and the gate in ion channels. Adv Protein Chem, 2003 63: p. 211–41. [PubMed: 12629972]
66. Bezanilla F, Voltage sensor movements. J Gen Physiol, 2002 120(4): p. 465–73. [PubMed: 12356849]
67. Bezanilla F, The voltage sensor in voltage-dependent ion channels. Physiol Rev, 2000 80(2): p. 555–92. [PubMed: 10747201]
68. Papazian DM and Bezanilla F, Voltage-dependent activation of ion channels. Adv Neurol, 1999 79: p. 481–91. [PubMed: 10514836]
69. Cha A and Bezanilla F, Structural implications of fluorescence quenching in the Shaker K+ channel. J Gen Physiol, 1998 112(4): p. 391–408. [PubMed: 9758859]

70. Sigg D and Bezanilla F, Total charge movement per channel. The relation between gating charge displacement and the voltage sensitivity of activation. J Gen Physiol, 1997 109(1): p. 27–39. [PubMed: 8997663]
71. Cha A and Bezanilla F, Characterizing voltage-dependent conformational changes in the Shaker K + channel with fluorescence. Neuron, 1997 19(5): p. 1127–40. [PubMed: 9390525]
72. Bezanilla F and Stefani E, Voltage-dependent gating of ionic channels. Annu Rev Biophys Biomol Struct, 1994 23: p. 819–46. [PubMed: 7522668]
73. Shenkel S and Bezanilla F, Patch recordings from the electrocytes of electrophorus. Na channel gating currents. J Gen Physiol, 1991 98(3): p. 465–78. [PubMed: 1662259]
74. Lee SY, et al., Structure of the KvAP voltage-dependent K+ channel and its dependence on the lipid membrane. Proc Natl Acad Sci U S A, 2005 102(43): p. 15441–6. [PubMed: 16223877]
75. Jiang QX, Wang DN, and MacKinnon R, Electron microscopic analysis of KvAP voltage-dependent K+ channels in an open conformation. Nature, 2004 430(7001): p. 806–10. [PubMed: 15306816]
76. Jiang Y, et al., The principle of gating charge movement in a voltage-dependent K+ channel. Nature, 2003 423(6935): p. 42–8. [PubMed: 12721619]
77. Jiang Y, et al., X-ray structure of a voltage-dependent K+ channel. Nature, 2003 423(6935): p. 33–41. [PubMed: 12721618]
78. Ahern CA, et al., Electrostatic contributions of aromatic residues in the local anesthetic receptor of voltage-gated sodium channels. Circ Res, 2008 102(1): p. 86–94. [PubMed: 17967784]
79. Horn R, How ion channels sense membrane potential. Proc Natl Acad Sci U S A, 2005 102(14): p. 4929–4930 1207. [PubMed: 15795366]
80. Ahern CA and Horn R, Focused electric field across the voltage sensor of potassium channels. Neuron, 2005 48(1): p. 25–9. [PubMed: 16202706]
81. Ahern CA and Horn R, Specificity of charge-carrying residues in the voltage sensor of potassium channels. J Gen Physiol, 2004 123(3): p. 205–16. [PubMed: 14769847]
82. Horn R, Coupled movements in voltage-gated ion channels. J Gen Physiol, 2002 120(4): p. 449–53. [PubMed: 12356847]
83. Horn R, A new twist in the saga of charge movement in voltage-dependent ion channels. Neuron, 2000 25(3): p. 511–4. [PubMed: 10774720]
84. Horn R, Conversation between voltage sensors and gates of ion channels. Biochemistry, 2000 39(51): p. 15653–8. [PubMed: 11123889]
85. Yang N and Horn R, Evidence for voltage-dependent S4 movement in sodium channels. Neuron, 1995 15(1): p. 213–8. [PubMed: 7619524]
86. Li Q, et al., Structural basis of lipid-driven conformational transitions in the KvAP voltage-sensing domain. Nat Struct Mol Biol, 2014 21(2): p. 160–6. [PubMed: 24413055]
87. Tang L, et al., Structural basis for Ca2+ selectivity of a voltage-gated calcium channel. Nature, 2014 505(7481): p. 56–61. [PubMed: 24270805]
88. Catterall WA, Structure and function of voltage-gated sodium channels at atomic resolution. Exp Physiol, 2014 99(1): p. 35–51. [PubMed: 24097157]
89. Payandeh J, et al., Crystal structure of a voltage-gated sodium channel in two potentially inactivated states. Nature, 2012 486(7401): p. 135–9. [PubMed: 22678296]
90. Catterall WA, Voltage-gated calcium channels. Cold Spring Harb Perspect Biol, 2011 3(8): p. a003947. [PubMed: 21746798]
91. Catterall WA, Ion channel voltage sensors: structure, function, and pathophysiology. Neuron, 2010 67(6): p. 915–28. [PubMed: 20869590]
92. Yarov-Yarovoy V, Baker D, and Catterall WA, Voltage sensor conformations in the open and closed states in ROSETTA structural models of K(+) channels. Proc Natl Acad Sci U S A, 2006 103(19): p. 7292–7. [PubMed: 16648251]
93. Sokolov S, Scheuer T, and Catterall WA, Ion permeation through a voltage-sensitive gating pore in brain sodium channels having voltage sensor mutations. Neuron, 2005 47(2): p. 183–9. [PubMed: 16039561]

94. Yu FH and Catterall WA, Overview of the voltage-gated sodium channel family. Genome Biol, 2003 4(3): p. 24.

95. Catterall WA, Structure and function of voltage-gated ion channels. Annu Rev Biochem, 1995 64: p. 493–531. [PubMed: 7574491]

96. Catterall WA, Molecular properties of voltage-sensitive sodium and calcium channels. Braz J Med Biol Res, 1988 21(6): p. 1129–44. [PubMed: 2855029]

97. Tombola F, Ulbrich MH, and Isacoff EY, Architecture and gating of Hv1 proton channels. J Physiol, 2009 587(Pt 22): p. 5325–9. [PubMed: 19915215]

98. Pathak MM, et al., Closing in on the resting state of the Shaker K(+) channel. Neuron, 2007 56(1): p. 124–40. [PubMed: 17920020]

99. Tombola F, Pathak MM, and Isacoff EY, How does voltage open an ion channel? Annu Rev Cell Dev Biol, 2006 22: p. 23–52. [PubMed: 16704338]

100. Tombola F, Pathak MM, and Isacoff EY, Voltage-sensing arginines in a potassium channel permeate and occlude cation-selective pores. Neuron, 2005 45(3): p. 379–88. [PubMed: 15694325]

101. Gandhi CS and Isacoff EY, Molecular models of voltage sensing. J Gen Physiol, 2002 120(4): p. 455–63. [PubMed: 12356848]

102. Mannuzzu LM and Isacoff EY, Independence and cooperativity in rearrangements of a potassium channel voltage sensor revealed by single subunit fluorescence. J Gen Physiol, 2000 115(3): p. 257–68. [PubMed: 10694254]

103. Mannuzzu LM, Moronne MM, and Isacoff EY, Direct physical measure of conformational rearrangement underlying potassium channel gating. Science, 1996 271(5246): p. 213–6. [PubMed: 8539623]

104. Larsson HP, et al., Transmembrane movement of the shaker K+ channel S4. Neuron, 1996 16(2): p. 387–397 1610. [PubMed: 8789953]

105. Heginbotham L, et al., Mutations in the K+ channel signature sequence. Biophys J, 1994 66(4): p. 1061–1067 1131. [PubMed: 8038378]

106. Heginbotham L and MacKinnon R, Conduction properties of the cloned Shaker K+ channel. Biophys J, 1993 65(5): p. 2089–2096 1130. [PubMed: 8298038]

107. Aggarwal SK and MacKinnon R, Contribution of the S4 segment to gating charge in the Shaker K + channel. Neuron, 1996 16(6): p. 1169–77. [PubMed: 8663993]

108. Starace DM and Bezanilla F, Histidine scanning mutagenesis of basic residues of the S4 segment of the shaker k+ channel. J Gen Physiol, 2001 117(5): p. 469–90. [PubMed: 11331357]

109. Seoh SA, et al., Voltage-sensing residues in the S2 and S4 segments of the Shaker K+ channel. Neuron, 1996 16(6): p. 1159–67. [PubMed: 8663992]

110. Islas LD and Sigworth FJ, Electrostatics and the gating pore of Shaker potassium channels. J Gen Physiol, 2001 117(1): p. 69–89. [PubMed: 11134232]

111. Islas LD and Sigworth FJ, Voltage sensitivity and gating charge in Shaker and Shab family potassium channels. J Gen Physiol, 1999 114(5): p. 723–42. [PubMed: 10539976]

112. Schoppa NE and Sigworth FJ, Activation of Shaker potassium channels. III. An activation gating model for wild-type and V2 mutant channels. J Gen Physiol, 1998 111(2): p. 313–342 2661. [PubMed: 9450946]

113. Schoppa NE, et al., The size of gating charge in wild-type and mutant Shaker potassium channels. Science, 1992 255(5052): p. 1712–5. [PubMed: 1553560]

114. Zhou Y and MacKinnon R, Ion binding affinity in the cavity of the KcsA potassium channel. Biochemistry, 2004 43(17): p. 4978–4982 3588. [PubMed: 15109256]

115. Zhou Y and MacKinnon R, The occupancy of ions in the K+ selectivity filter: charge balance and coupling of ion binding to a protein conformational change underlie high conduction rates. J Mol Biol, 2003 333(5): p. 965–975 3587. [PubMed: 14583193]

116. Zhang X, et al., Crystal structure of an orthologue of the NaChBac voltage-gated sodium channel. Nature, 2012 486(7401): p. 130–4. [PubMed: 22678295]

117. Takeshita K, et al., X-ray crystal structure of voltage-gated proton channel. Nat Struct Mol Biol, 2014 21(4): p. 352–7. [PubMed: 24584463]

118. Clayton GM, et al., Combining electron crystallography and X-ray crystallography to study the MlotiK1 cyclic nucleotide-regulated potassium channel. J Struct Biol, 2009 167(3): p. 220–6. [PubMed: 19545635]
119. Tao X, Hite RK, and MacKinnon R, Cryo-EM structure of the open high-conductance Ca2+-activated K+ channel. Nature, 2017 541(7635): p. 46–51. [PubMed: 27974795]
120. Hite RK, Tao X, and MacKinnon R, Structural basis for gating the high-conductance Ca2+-activated K+ channel. Nature, 2017 541(7635): p. 52–57. [PubMed: 27974801]
121. Fox PD, Loftus RJ, and Tamkun MM, Regulation of Kv2.1 K(+) conductance by cell surface channel density. J Neurosci, 2013 33(3): p. 1259–70. [PubMed: 23325261]
122. O'Connell KM, Loftus R, and Tamkun MM, Localization-dependent activity of the Kv2.1 delayed-rectifier K+ channel. Proc Natl Acad Sci U S A, 2010 107(27): p. 12351–6. [PubMed: 20566856]
123. O'Connell KM and Tamkun MM, Targeting of voltage-gated potassium channel isoforms to distinct cell surface microdomains. J Cell Sci, 2005 118(Pt 10): p. 2155–66. [PubMed: 15855232]
124. Martens JR, et al., Isoform-specific localization of voltage-gated K+ channels to distinct lipid raft populations. Targeting of Kv1.5 to caveolae. J Biol Chem, 2001 276(11): p. 8409–14. [PubMed: 11115511]
125. Purcell EK, et al., Cholesterol influences voltage-gated calcium channels and BK-type potassium channels in auditory hair cells. PLoS ONE, 2011 6(10): p. e26289. [PubMed: 22046269]
126. Huang CW, Wu YJ, and Wu SN, Modification of activation kinetics of delayed rectifier K+ currents and neuronal excitability by methyl-beta-cyclodextrin. Neuroscience, 2011 176: p. 431–41. [PubMed: 21073928]
127. Finol-Urdaneta RK, et al., Modulation of KvAP unitary conductance and gating by 1-alkanols and other surface active agents. Biophys J, 2010 98(5): p. 762–72. [PubMed: 20197029]
128. Guo J, et al., Effects of cholesterol levels on the excitability of rat hippocampal neurons. Mol Membr Biol, 2008 25(3): p. 216–23. [PubMed: 18428037]
129. Pottosin II, et al., Methyl-beta-cyclodextrin reversibly alters the gating of lipid rafts-associated Kv1.3 channels in Jurkat T lymphocytes. Pflugers Arch, 2007 454(2): p. 235–44. [PubMed: 17242956]
130. Balijepalli RC, et al., Kv11.1 (ERG1) K+ channels localize in cholesterol and sphingolipid enriched membranes and are modulated by membrane cholesterol. Channels (Austin), 2007 1(4): p. 263–72. [PubMed: 18708743]
131. Abi-Char J, et al., Membrane cholesterol modulates Kv1.5 potassium channel distribution and function in rat cardiomyocytes. J Physiol, 2007 582(Pt 3): p. 1205–17. [PubMed: 17525113]
132. Xia F, et al., Disruption of pancreatic beta-cell lipid rafts modifies Kv2.1 channel gating and insulin exocytosis. J Biol Chem, 2004 279(23): p. 24685–91. [PubMed: 15073181]
133. Pouvreau S, et al., Membrane cholesterol modulates dihydropyridine receptor function in mice fetal skeletal muscle cells. J Physiol, 2004 555(Pt 2): p. 365–81. [PubMed: 14724204]
134. Hajdu P, et al., Cholesterol modifies the gating of Kv1.3 in human T lymphocytes. Pflugers Arch, 2003 445(6): p. 674–82. [PubMed: 12632187]
135. Rudakova E, et al., Localization of Kv4.2 and KChIP2 in lipid rafts and modulation of outward K + currents by membrane cholesterol content in rat left ventricular myocytes. Pflugers Arch, 2015 467(2): p. 299–309. [PubMed: 24793047]
136. Bowles DK, et al., Hypercholesterolemia inhibits L-type calcium current in coronary macro-, not microcirculation. J Appl Physiol (1985), 2004 96(6): p. 2240–8. [PubMed: 14752123]
137. Heaps CL, Tharp DL, and Bowles DK, Hypercholesterolemia abolishes voltage-dependent K+ channel contribution to adenosine-mediated relaxation in porcine coronary arterioles. Am J Physiol Heart Circ Physiol, 2005 288(2): p. H568–76. [PubMed: 15458946]
138. Balajthy A, et al., 7DHC-induced changes of Kv1.3 operation contributes to modified T cell function in Smith-Lemli-Opitz syndrome. Pflugers Arch, 2016.
139. Chun YS, et al., Cholesterol modulates ion channels via down-regulation of phosphatidylinositol 4,5-bisphosphate. J Neurochem, 2010 112(5): p. 1286–94. [PubMed: 20015154]

140. Coyan FC, et al., A long QT mutation substitutes cholesterol for phosphatidylinositol-4,5-bisphosphate in KCNQ1 channel regulation. PLoS One, 2014 9(3): p. e93255. [PubMed: 24681627]
141. Heaps CL, et al., Effects of exercise training and hypercholesterolemia on adenosine activation of voltage-dependent K+ channels in coronary arterioles. J Appl Physiol, 2008 105(6): p. 1761–71. [PubMed: 18832757]
142. Balijepalli SY, et al., Mechanism of loss of Kv11.1 K+ current in mutant T421M-Kv11.1-expressing rat ventricular myocytes: interaction of trafficking and gating. Circulation, 2012 126(24): p. 2809–18. [PubMed: 23136156]
143. Xu Y, Ramu Y, and Lu Z, Removal of phospho-head groups of membrane lipids immobilizes voltage sensors of K+ channels. Nature, 2008 451(7180): p. 826–9. [PubMed: 18273018]
144. Ramu Y, Xu Y, and Lu Z, Enzymatic activation of voltage-gated potassium channels. Nature, 2006 442(7103): p. 696–9. [PubMed: 16799569]
145. Zheng H, et al., Lipid-dependent gating of a voltage-gated potassium channel. Nat Commun, 2011 2: p. 250. [PubMed: 21427721]
146. Jiang Q-X and Gonen T, The influence of lipids on voltage-gated ion channels. Curr Opin Struct Biol, 2012 22: p. 529–36. [PubMed: 22483432]
147. Gantz SC and Bean BP, Cell-Autonomous Excitation of Midbrain Dopamine Neurons by Endocannabinoid-Dependent Lipid Signaling. Neuron, 2017 93(6): p. 1375–1387 e2. [PubMed: 28262417]
148. Randich AM, et al., Biochemical and structural analysis of the hyperpolarization-activated K(+) channel MVP. Biochemistry, 2014 53(10): p. 1627–36. [PubMed: 24490868]
149. Amsalem M, et al., Membrane cholesterol depletion as a trigger of Nav1.9 channel-mediated inflammatory pain. EMBO J, 2018 37(8).
150. Calhoun JD and Isom LL, The role of non-pore-forming beta subunits in physiology and pathophysiology of voltage-gated sodium channels. Handb Exp Pharmacol, 2014 221: p. 51–89. [PubMed: 24737232]
151. Hofmann F, Belkacemi A, and Flockerzi V, Emerging Alternative Functions for the Auxiliary Subunits of the Voltage-Gated Calcium Channels. Curr Mol Pharmacol, 2015 8(2): p. 162–8. [PubMed: 25966689]
152. Liu SL, et al., Orthogonal lipid sensors identify transbilayer asymmetry of plasma membrane cholesterol. Nat Chem Biol, 2017 13(3): p. 268–274. [PubMed: 28024150]
153. Lingwood D and Simons K, Lipid rafts as a membrane-organizing principle. Science, 2010 327(5961): p. 46–50. [PubMed: 20044567]
154. Kaiser HJ, et al., Order of lipid phases in model and plasma membranes. Proc Natl Acad Sci U S A, 2009 106(39): p. 16645–50. [PubMed: 19805351]
155. Coskun U and Simons K, Membrane rafting: From apical sorting to phase segregation. FEBS Lett, 2009 28: p. 28.
156. Anderson RG, The caveolae membrane system. Annu Rev Biochem, 1998 67: p. 199–225. [PubMed: 9759488]
157. Anderson RG, Transendothelial movement and caveolae. Nat Biotechnol, 2008 26(4): p. 380–1; author reply 381–2. [PubMed: 18392012]
158. Mizuno H, et al., Fluorescent probes for superresolution imaging of lipid domains on the plasma membrane. Chem. Sci, 2011 2.
159. Klitzing HA, Weber PK, and Kraft ML, Secondary ion mass spectrometry imaging of biological membranes at high spatial resolution. Methods Mol Biol, 2013 950: p. 483–501. [PubMed: 23086891]
160. Kraft ML, Sphingolipid Organization in the Plasma Membrane and the Mechanisms That Influence It. Front Cell Dev Biol, 2016 4: p. 154. [PubMed: 28119913]
161. Richard M and Raquel F, Non-raft forming sphingomyelin-cholesterol mixtures. Chemistry and physics of lipids 2004 132(1): p. 37–46. [PubMed: 15530446]
162. Dietrich C, et al., Lipid rafts reconstituted in model membranes. Biophys J, 2001 80(3): p. 1417–28. [PubMed: 11222302]

163. Wang L, Bose PS, and Sigworth FJ, Using cryo-EM to measure the dipole potential of a lipid membrane. Proc Natl Acad Sci U S A, 2006 103(49): p. 18528–33. [PubMed: 17116859]
164. Nyholm TK, et al., Construction of a DOPC/PSM/Cholesterol Phase Diagram Based on the Fluorescence Properties of trans-Parinaric Acid. Langmuir, 2011.
165. Kolter T and Sandhoff K, Sphingolipid metabolism diseases. Biochim Biophys Acta, 2006 1758(12): p. 2057–79. [PubMed: 16854371]
166. Cheng SH, Gene therapy for the neurological manifestations in lysosomal storage disorders. J Lipid Res, 2014.
167. Bolsover FE, et al., Cognitive dysfunction and depression in Fabry disease: a systematic review. J Inherit Metab Dis, 2014 37(2): p. 177–87. [PubMed: 23949010]
168. Bellettato CM and Scarpa M, Pathophysiology of neuropathic lysosomal storage disorders. J Inherit Metab Dis, 2010 33(4): p. 347–62. [PubMed: 20429032]
169. Millard EE, et al., The sterol-sensing domain of the Niemann-Pick C1 (NPC1) protein regulates trafficking of low density lipoprotein cholesterol. J Biol Chem, 2005 280(31): p. 28581–90. [PubMed: 15908696]
170. Millard EE, et al., Niemann-pick type C1 (NPC1) overexpression alters cellular cholesterol homeostasis. J Biol Chem, 2000 275(49): p. 38445–51. [PubMed: 10964915]
171. Praggastis M, et al., A murine Niemann-Pick C1 I1061T knock-in model recapitulates the pathological features of the most prevalent human disease allele. J Neurosci, 2015 35(21): p. 8091–106. [PubMed: 26019327]
172. Andersson M, et al., Structural dynamics of the S4 voltage-sensor helix in lipid bilayers lacking phosphate groups. J Phys Chem B, 2011 115(27): p. 8732–8. [PubMed: 21692541]
173. O'Connell KM, Martens JR, and Tamkun MM, Localization of ion channels to lipid Raft domains within the cardiovascular system. Trends Cardiovasc Med, 2004 14(2): p. 37–42. [PubMed: 15030787]
174. Martens JR, O'Connell K, and Tamkun M, Targeting of ion channels to membrane microdomains: localization of KV channels to lipid rafts. Trends Pharmacol Sci, 2004 25(1): p. 16–21. [PubMed: 14723974]
175. Martens JR, et al., Differential targeting of Shaker-like potassium channels to lipid rafts. J Biol Chem, 2000 275(11): p. 7443–6. [PubMed: 10713042]
176. Bichenkov E and Ellingson JS, Temporal and quantitative expression of the myelin-associated lipids, ethanolamine plasmalogen, galactocerebroside, and sulfatide, in the differentiating CG-4 glial cell line. Neurochem Res, 1999 24(12): p. 1549–56. [PubMed: 10591405]
177. Unwin N, Segregation of lipids near acetylcholine-receptor channels imaged by cryo-EM. IUCrJ, 2017 4(Pt 4): p. 393–399.
178. Sun J, Comeau JF, and Baenziger JE, Probing the structure of the uncoupled nicotinic acetylcholine receptor. Biochim Biophys Acta, 2017 1859(2): p. 146–154.
179. Brannigan G, Direct Interactions of Cholesterol With Pentameric Ligand-Gated Ion Channels: Testable Hypotheses From Computational Predictions. Curr Top Membr, 2017 80: p. 163–186. [PubMed: 28863815]
180. daCosta CJ, et al., A distinct mechanism for activating uncoupled nicotinic acetylcholine receptors. Nat Chem Biol, 2013 9(11): p. 701–7. [PubMed: 24013278]
181. Barrantes FJ, Cell-surface translational dynamics of nicotinic acetylcholine receptors. Front Synaptic Neurosci, 2014 6: p. 25. [PubMed: 25414663]
182. Gao Y, et al., TRPV1 structures in nanodiscs reveal mechanisms of ligand and lipid action. Nature, 2016 534(7607): p. 347–51. [PubMed: 27281200]

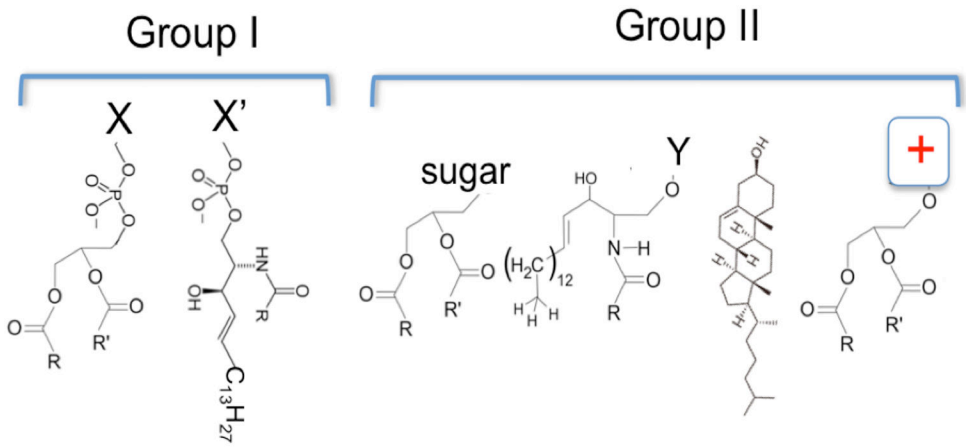

Figure 1: Two main groups of lipid molecules in eukaryotic cell membranes.

Group I are phospholipids, include 1) glycerol-phospholipids. The group X could be choline (PC), ethanolamine (PE), glycerol (PG), serine (PS), inositol (PIs), or proton (PA). 2) Sphingosine phospholipids. Group X' refers to mainly choline.

Group II are non-phospholipids, and include 3) glycerol-glycolipids; 4) Sphingosine-glycolipids. Group Y represents different sugar groups, mono-saccharides or oligo-saccharides. 5) Cholesterol (CHOL). 6) Cationic glycerol-lipids.

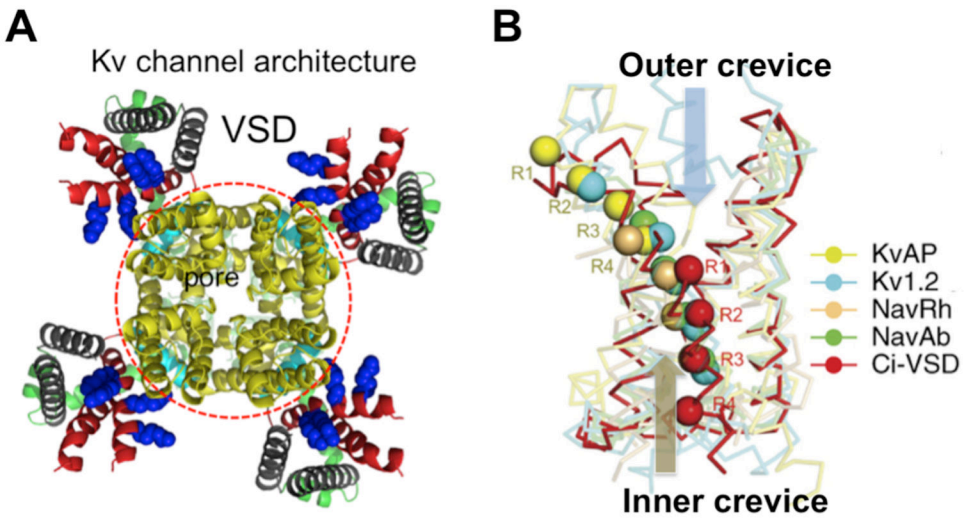

Figure 2: Architecture of a Kv channel and variations in VSD structures.

A) KvAP model after the Kv2.1 structure showing a central pore domain (red circle) and four VSDs. **B)** Five VSD structures in alignment. Arginine residues on S4 are aligned across the gating pore. Outer (upper) and inner (lower) crevices separated by a hydrophobic gasket (red). In a full resting (down) state, all four Arg residues move to the inner crevice, and drive the pore domain into the closed state [1, 2]. Panel B was modified from ref 1.

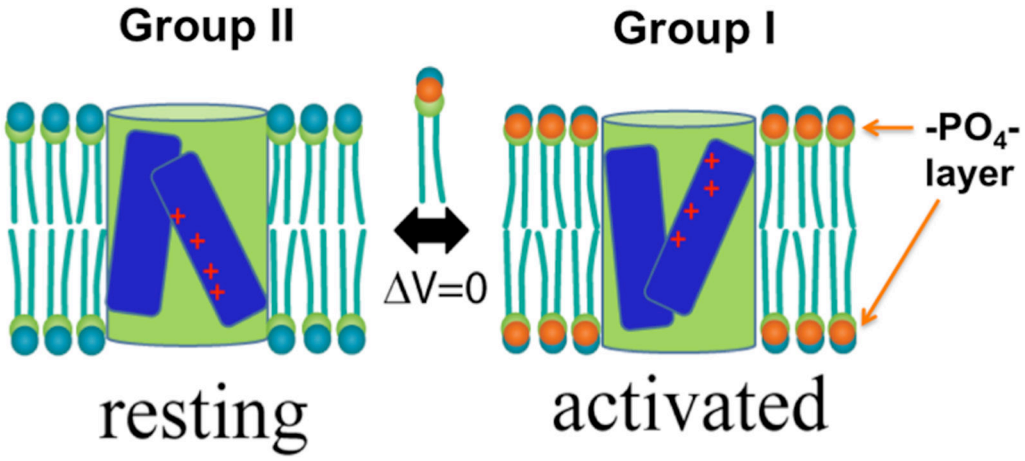

Figure 3: Simplified scheme for lipid-dependent gating.

A VSD (blue bars with + charges in red) flanking a pore domain (green cylinder) switches between resting (“down” state of the VSDs) and activated (“up” state of the VSDs) state in Group II and Group I lipids at ΔV=0, showing the inner and outer crevices of the gating pore. The pore is assumed to take an inward-facing conformation in the resting state and an out-ward-facing conformation in the activated state.

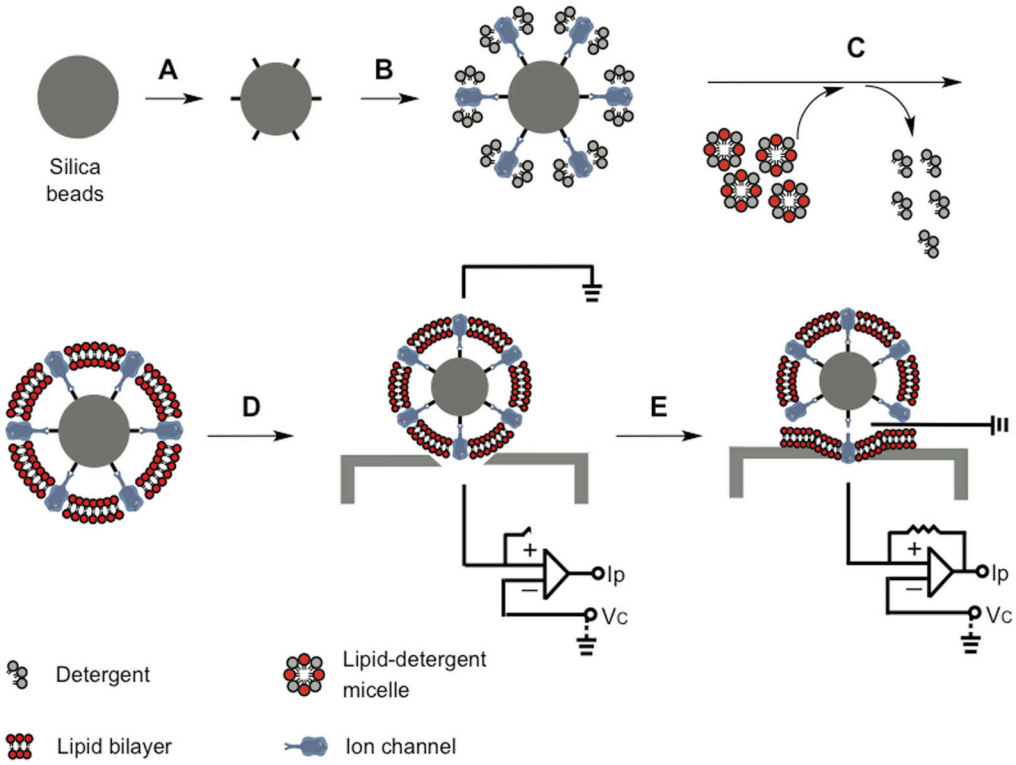

Figure 4: bSUMs for preferred directional insertion of ion channels in CHOL-rich membranes.
Chemical functionalization added ligand to the surface of silica beads (A). Channels bind to the ligands and orient themselves (B). Addition of detergent-solubilized lipids and slow removal of the detergents by BioBeads leads to the formation of one bilayer membranes around each bead (D), which is the bSUM. The channels in bSUMs can be patched using a planar glass electron for electrical recordings (E). Adapted from ref [3].

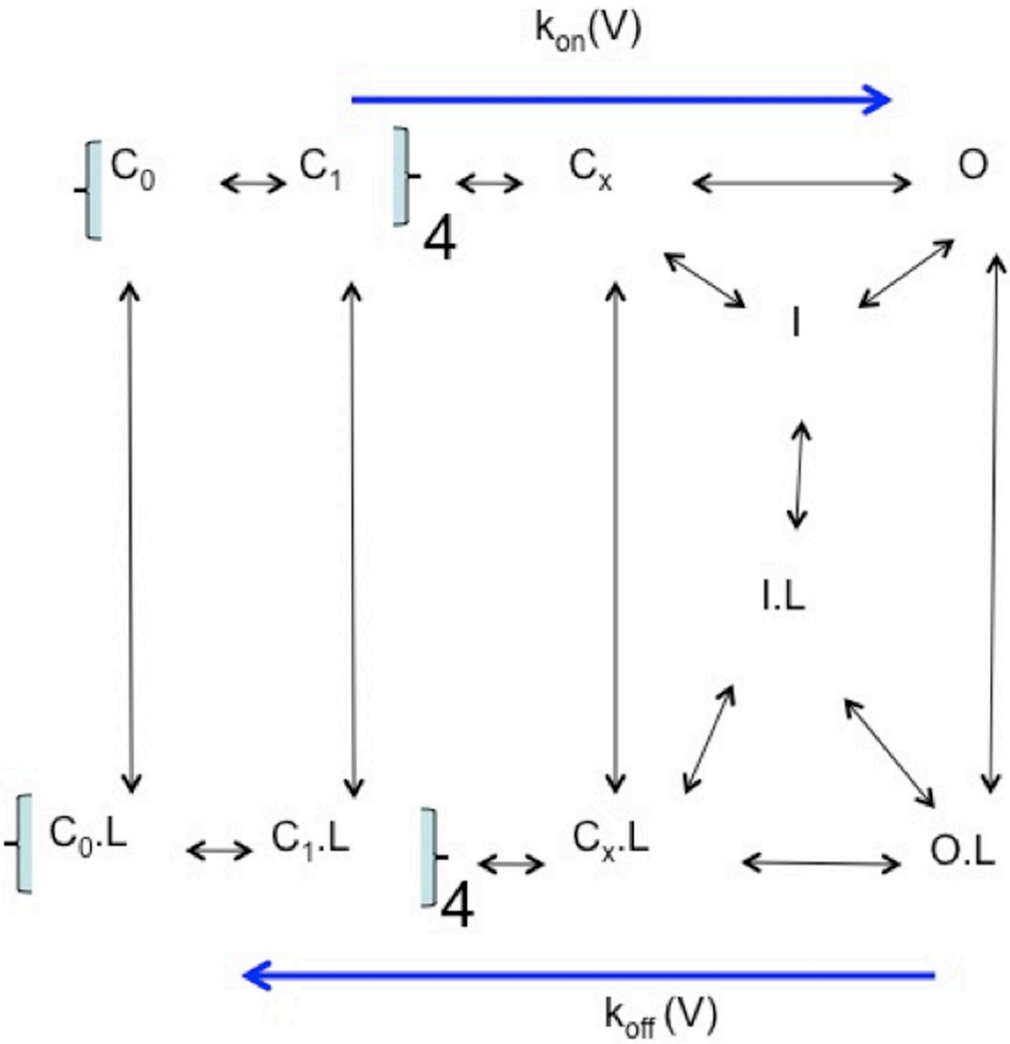

Figure 5: A gating model for CHOL-dependent gating.

The fully resting state (C_0) switches to C_1 states in four independent steps because of four VSDs. The concerted coupling between four VSDs leads to the closed state immediately before the channel opening (C_x). The open state (O) can become inactivated (I) so as the closed state (C_x as an example). Cholesterol as the ligand (L) can be partitioned around channels in each state. The measured activation rate [$k_{on}(V)$] will be determined by the forward rate-limiting step. The deactivation rate [$k_{off}(V)$] will be determined by the closing rate of O.

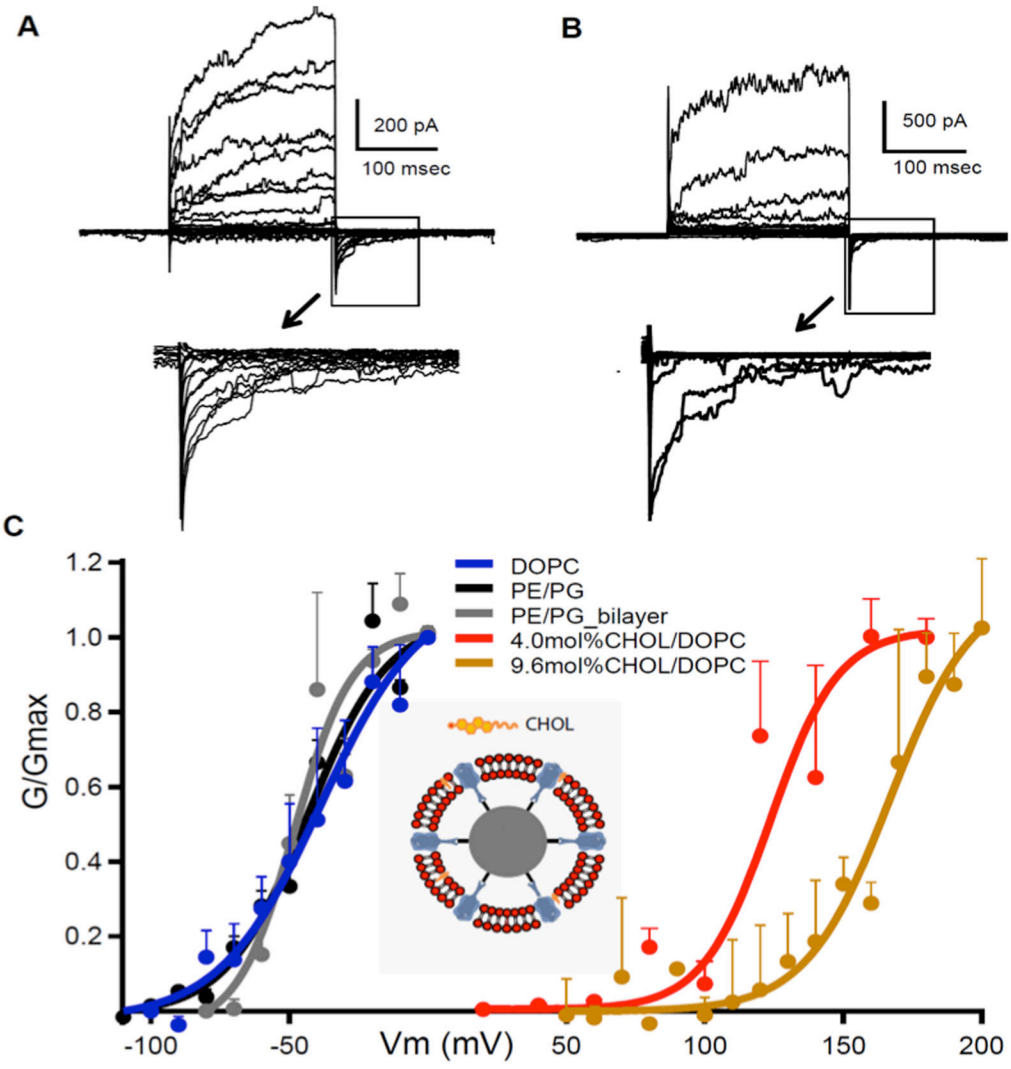

Figure 6: CHOL inhibits KvAP in bSUMs.

A) Activity of KvAP in bSUMs made of PE:PG (3:1), pulsed from −160 to 180mV at 10 mV steps. **B**) Recordings from KvAP channels in bSUMs made of DOPC with 9.6 mol% of CHOL. **C**) G-V for KvAP in bSUMs of DOPC (blue; n=3), PE:PG (3:1, black; n=4), DOPC/CHOL (4.0 mol% in red and 9.6% in brown; n=3) and PE/PG 3:1 BLMs (grey; n=3). Boltzmann fittings (solid lines) yielded ($Z\delta$, $V_{1/2}$) (e_0, mV) for channels in BLM (3.0, −47.5), PE/PG bSUMs (2.0,−45), DOPC bSUMs (1.6, −42.0), 4.0 mol% CHOL (1.6, 118) and 9.6 mol% CHOL (2.0,162) in DOPC bSUMs. Error bars: s.d.